

Cite this: *Soft Matter*, 2012, **8**, 8483www.rsc.org/softmatter

PAPER

Creep and recovery behaviors of magnetorheological plastomer and its magnetic-dependent properties

Yangguang Xu,^a Xinglong Gong,^{*a} Shouhu Xuan,^{*a} Xiaofeng Li,^a Lijun Qin^a and Wanquan Jiang^b

Received 28th April 2012, Accepted 7th June 2012

DOI: 10.1039/c2sm25998b

The creep and recovery behaviors of magnetorheological plastomer (MRP) were systematically investigated to further understand its deformation mechanism under constant stress. The experimental results suggested that the time-dependent mechanical properties of MRP were highly dependent on the magnetic field and the magnetic-controllable mechanism was discussed. The influences of iron particle distribution and temperature on the creep and recovery behaviors in the absence and presence of a magnetic field were investigated, respectively. A great discrepancy was presented in creep curves for the isotropic and anisotropic MRP under an external magnetic field, which must be induced by the different particle assemblies. In addition, the creep strain of MRP tended to decrease with increasing temperature under a 930 mT magnetic field and this phenomenon was opposite to the results obtained without a magnetic field. Finally, a hypothesis was proposed to explain the temperature effect on the creep behaviors of MRP.

1. Introduction

Creep, the variation of strain with time when a constant stress is applied to the sample, is a time-dependent mechanical behavior of materials. If the stress is instantaneously removed, the dependence of strain on time is defined as the recovery behavior. On the one hand, the microstructure evolution of viscoelastic materials can be deduced from creep and recovery experiments, which is helpful to understand the mechanism behind the rheological properties of materials. On the other hand, the theoretical research of creep models has still attracted people's attention in recent years.^{1–3} With these models, the response of material to arbitrary load can be predicted. However, the material functions (such as creep compliance or relaxation modulus) in these constitutive equations need to be obtained by experimental methods. Furthermore, creep and recovery properties are also very important for some engineering applications. For example the creep compliance and recovery ratio are the critical assessment parameters for structure elements which are maintained under constant load.

Creep and recovery techniques have been widely used to investigate the deformation mechanism of polymer melts,⁴ Nafion,⁵ PMMA–nanoclay composites,⁶ recombinant protein polymers,⁷ gelled waxy oil,⁸ polypropylene–carbon nanotube

composites,⁹ and so on. By combining the creep data and other experimental results, the mechanical properties of materials can be further analyzed. Riggleman *et al.* explored the nonlinear creep response of a model polymer glass under tension and compression with molecular dynamics simulations, where the structure of the material was examined as a time-dependent function.¹⁰ Awasthi and Joshi carried out creep and oscillatory experiments on soft glassy materials at different temperatures. The temperature dependent creep time–aging time superposition enables the estimation of long time rheological behavior at low temperatures and high ages by carrying out short time tests at high temperatures and small ages.¹¹ By modifying the effective time scale, the time–aging time–stress superposition can be obtained from the time–aging time superposition at different stresses. The time–aging time–stress superposition demonstrates greater predictive capacity in comparison to that from the time–aging time superposition at a single stress.¹² Dynamical parameters in Langmuir polymer films can be obtained from creep compliance experiments carried out by Hilles and Monroy, by which guidance was provided to explore the non-linear dynamics of Langmuir polymer films.¹³

However, the investigation on the creep and recovery behaviors of MR materials is rare, though it is helpful to understand their deformation mechanism.^{14–17} Li *et al.* found that the response strain of MR fluids is highly dependent on the constant stress level. The creep behaviors of MR fluids are complex and can not be explained by the ideal single-particle-width chain model. Then, a thick column structure hypothesis was proposed to explain the complex creep behaviors.¹⁴ A similar conclusion was drawn by See *et al.* They attributed the mechanical behavior which can not be described by Bingham fluid equation to the

^aCAS Key Laboratory of Mechanical Behavior and Design of Materials, Department of Modern Mechanics, University of Science and Technology of China (USTC), Hefei, Anhui, China. E-mail: gongxl@ustc.edu.cn; xuansh@ustc.edu.cn; Fax: +86 551 3600419; +86 551 3600419; Tel: +86 551 3600419; +86 551 3606382

^bDepartment of Chemistry, University of Science and Technology of China, Hefei, Anhui, China

local concentrations of stress caused by the irregular configuration of the particles within the aggregates when an external stress is applied.¹⁶ In addition, both experimental and modeling studies of the creep and recovery behaviors of MR elastomers were also investigated by Li *et al.* The results of their experiment indicated that the creep and recovery behaviors of MR elastomers are far different from those of MR fluids.¹⁷

MR gels can be regarded as an intermediate state between MR fluids and MR elastomers, which were firstly developed to solve the particle sedimentation of MR fluids.¹⁸ Adding proper amount of polymer into the carrier liquid can increase the stability of MR fluids effectively. These MR gels are prepared by adding polymer into the carrier liquid with a liquid-like state and show better stability than MR fluids.^{19–24} Very recently, a novel solid-like MR gel which exhibited high MR performance was developed and no particle sedimentation existed in this solid-like MR gel.^{25–27} Due to the soft polymer matrix, stable chain-like microstructures of the solid-like MR gels can be kept even after removing the external magnetic field and the soft magnetic particles can be rearranged by applying an external magnetic field in a different direction. The rearrangement of particles will change the magnetorheological performance of MR materials, which is important in studying their microstructure mechanism and in some applications. These unique properties broaden the application of MR materials, thus further investigations on the solid-like MR gels are necessary. The creep and recovery behaviors of solid-like MR gels are much more helpful to further understand the magnetic-dependent properties on the rheological properties of MR materials. To our knowledge, the deformation mechanism of the solid-like MR gels under constant stress has not been considerably researched and this is the motivation of this study.

In this work, the influences of creep time, constant stress level, magnetic field, particle distribution, temperature, and their coupling effects on the creep and recovery behaviors of MR elastomer²⁸ (MRP, which is actually a kind of solid-like gels) were systematically investigated. The reasons for the different time-dependent mechanical behavior affected by different influence factor were discussed. Especially, a discussion was conducted to analyze the temperature effect on the creep behaviors of MRP which is far different from MR fluids and MR elastomers.

2. Experimental

2.1. Synthesis of MR plastomers

The plastic matrix of MRP was synthesized by a chemical method. Toluene diisocyanate (TDI, 2,4- \approx 80%, 2,6- \approx 20%, Tokyo Chemical Industry Co., Ltd, Japan) and polypropylene glycol (PPG-1000, $M_n = 1000$, Sigma-Aldrich (Shanghai) Trading Co., Ltd, China) with a molar ratio of 3 : 1 were added into a three-necked round bottom flask (with a stirrer that agitated the reactants vigorously all the time through the middle neck of the flask) at 75 °C for 2 hours. 1,4-Butanediol (BDO, Sinopharm Chemical Reagent Co., Ltd, China) was then added as a chain extender after lowering the temperature to 65 °C. Eqn (1) can be used to calculate the weight of BDO.

$$m_{\text{BDO}} = 90.12 \text{ g mol}^{-1} \times \left(\frac{m_{\text{TDI}}}{174.15 \text{ g mol}^{-1} \times 1.1} - \frac{m_{\text{PPG}}}{1000 \text{ g mol}^{-1}} \right) \quad (1)$$

Where m_{BDO} , m_{TDI} , and m_{PPG} indicate the weight of BDO, TDI, and PPG, respectively. 1 h later, a small quantity (about 0.15 g) of stannous octoate (Sinopharm Chemical Reagent Co., Ltd, China) was dropped into the reactants to accelerate the cross linking reaction. The synthesis process finished after the catalyst (stannous octoate) was added for about 20 min. In addition, acetone (Sinopharm Chemical Reagent Co., Ltd, China) was added to avoid gelation during the reaction.

Once the matrix (in fact, the matrix is mainly composed of plastic polyurethane) was synthesized, quantitative carbonyl iron particles (type CN, provided by BASF in Germany with an average radius of 6 μm) with weight fraction of 70% were added into it immediately before the matrix cooled down. After vigorously stirring for a long enough time until the matrix and iron particles were well mixed, the product was placed at room temperature for a week before testing. For the freshly prepared MRP, the iron particles are distributed in the matrix randomly, and this kind of MRP was named as isotropic MRP. If the isotropic MRP is subjected to a magnetic field of 800 mT for 10 min, the iron particles will move along the direction of magnetic field and form chain-like or column-like structures. The MRP with chain-like or column-like structures is defined as anisotropic MRP. It is worthy to note that except for Section 3.4, the MRP that we mentioned in this work refers to anisotropic MRP.

2.2. Experimental technique

A parallel-plate rheometer (Physica MCR 301, Anton Paar Co., Austria) equipped with a MR accessory (MRD 180) was used to measure the creep and recovery behaviors of MRP and their magnetic field correlation. The magnetic field strength can be controlled by a power supply unit PS-DC/MRD which is connected to the MRD 180. The sample with 20 mm diameter and 1 mm thickness was placed between the rotor and the bed. It should be noted that the data recording method was set from “measuring point duration” menu in the measurement window. “Variable measuring point duration log” option was selected as the interval setting during creep and recovery tests. With this interval setting method, the measuring point duration varies in logarithmic distribution from the initial point duration to the last point duration. Here, the initial point duration was set as 0.01 s while the last point duration was set as 25 s. The total length of the interval which is displayed underneath the “time unit” menu is calculated automatically according to the number of data points and the point durations. This interval setting method not only records the initial details of creep and recovery behaviors, but also makes the amount of data points not so large at a long enough experimental time.

An ideal creep and recovery experiment is illustrated schematically in Fig. 1. A constant stress ($\tau_0 = PK$) is applied instantaneously to the sample, after a setting creep time the stress is removed suddenly. At the same time, the response strain to the stress varying with time is recorded. Plenty information about viscoelastic properties of materials can be analyzed from creep

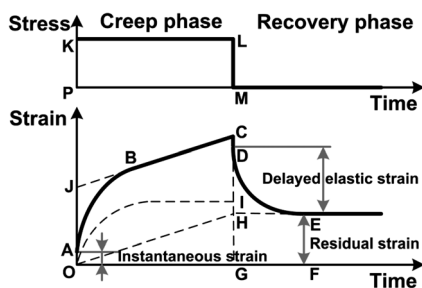


Fig. 1 Typical creep and recovery curve of linear viscoelastic materials under a constant stress.

and recovery curves. Fig. 1 shows a typical creep and recovery curve for linear viscoelastic materials.

OA represents the creep instantaneous strain γ_{in} which reflects the elastic properties of materials. In fact, the real instantaneous strain can not be obtained experimentally because it needs time for the device to record data and the instantaneous strain usually generates less than 10^{-10} s. This term is often used to present either the strain when the first reading is taken or the strain obtained from a rather dubious extrapolation of measured strains to $t = 0$. The shortest useful measuring time is equal to the propagation time of wave according to the suggestion made by Whorlow.²⁹ In our study, the recording time for the first data point was set as 0.01 s. It is obvious that this time is far longer than the propagation time of the wave. Limited to the experimental technique, we regard the first data point as the instantaneous strain, and this datum is larger than the real instantaneous strain. The deviation between the two values is difficult to confirm and it is not the emphasis in this study. If the constant stress is removed, an instantaneous recovery strain CD (γ_e) will generate and this instantaneous recovery strain is usually equal to the creep instantaneous strain, *i.e.* $\gamma_e = \gamma_{in}$.

The strain usually increases nonlinearly (AB) with the time of applying stress at first, and eventually a linear region (BC) will appear. AB is referred to as the delayed elastic strain which can be fully recovered. BC is an irreversible component of strain. This component, which is defined as the viscous flow, will increase linearly with time for linear viscoelastic materials. In the recovery phase, the delayed elastic strain will decrease to zero (DE) with time gradually and the viscous flow component (BC) will be kept. For ideal linear viscoelastic materials, if we decompose the curve ABC into OI and OH, where OI represents delayed elastic strain component and OH represents viscous flow component, the residual strain (EF) is equal to GH, which means no plastic component is included in the residual strain. However, for most real materials, the time-dependent mechanical behaviors are more complex than those described in Fig. 1. Especially for viscoelastic-plastic materials, the plastic component will appear in the creep stage, which will lead to complex nonlinear effects. The plastic component is also an unrecoverable strain, so it will be included in the residual strain and it can be estimated by subtracting the viscous flow component from the residual strain (*i.e.* plastic strain = EF – GH).

Based on the experimental data, the creep and recovery curves can be fitted by Burger's model³⁰ and Weibull distribution function³¹ respectively. The fitting parameters obtained from these two models can help us to determine the component of

creep strain, which is useful to analyze the deformation mechanism of materials. Burger's model, which combines Maxwell and Kelvin–Voigt elements, is frequently used to predict the creep behavior of composites. The creep strain (γ_T) consists of instantaneous strain (γ_{in}), delayed elastic strain (γ_{de}), and residual strain (γ_{re}), which can be represented as a function of time as follows:

$$\gamma_T = \gamma_{in} + \gamma_{de} + \gamma_{re} \quad (2)$$

$$\gamma_T(t) = \tau_0 \left[\frac{1}{G_M} + \frac{1}{\eta_M} (1 - e^{-G_K t / \eta_K}) + \frac{t}{\eta_M} \right] = J(t) \cdot \tau_0 \quad (3)$$

Where t , τ_0 denote the loading time and constant stress respectively, G_M , η_M , G_K , and η_K represent the modulus of the Maxwell spring, the viscosity of Maxwell dashpot, the modulus of the Kelvin spring, and the viscosity of the Kelvin dashpot, respectively. $J(t)$ is defined as the ratio of creep strain to constant stress and is called the creep compliance. Creep compliance is an important parameter to characterize the creep behavior of materials. The Weibull distribution function can be used to describe the recovery behavior after unloading. The time-dependent recovery strain (γ_R) is expressed as:

$$\gamma_R(t) = \gamma_{er} \left[\exp \left(- \left(\frac{t - t_0}{\eta_r} \right)^{\alpha_r} \right) \right] + \gamma_{re} \quad (4)$$

Here, γ_{er} , which is determined by the constant parameter η_r , α_r is the delayed elastic strain and γ_{re} is the residual strain in the recovery stage. t_0 denotes the recovery time. In this work, the non-linear curve fitting function of OriginPro 8.0 software was used to determine the parameters in the two phenomenon models.

3. Results and discussion

3.1. Determination of creep time

A series of creep and recovery experiments at different creep times under a 930 mT magnetic field and a 20 kPa constant shear stress were firstly carried out (Fig. 2a). The five creep curves are well superposed, indicating good experimental repeatability and reliability. The creep curves bend downwards at first (this region is defined as primary creep) and then are proportional to time (this region is defined as secondary creep). No tertiary creep in which deformation accelerates until creep rupture occurs is observed from the creep curves even at the longest creep time of 7200 s. The instantaneous strain (which is smaller than the first recorded point) can be neglected in comparison to the delayed elastic strain (which can be calculated from recovery curves) and the residual strain (*i.e.* unrecoverable strain, which can also be read from recovery curves). Clearly, the above observation is far different from the creep behaviors of MR fluids¹⁴ and MR elastomers.¹⁷ There is no definable boundary between primary creep and secondary creep,²⁹ but it is obvious that the time for the formation of delayed elastic strain is longer than MR fluids and MR elastomers, which is relevant with the stretching of the soft chain segments of polyurethane in MRP. Accordingly, the delayed elastic strain can be totally recovered in the recovery phase at long enough times, which is attributed to the convolution of soft chain segments after the applied stress is removed. In addition, the delayed elastic strains are almost the same at

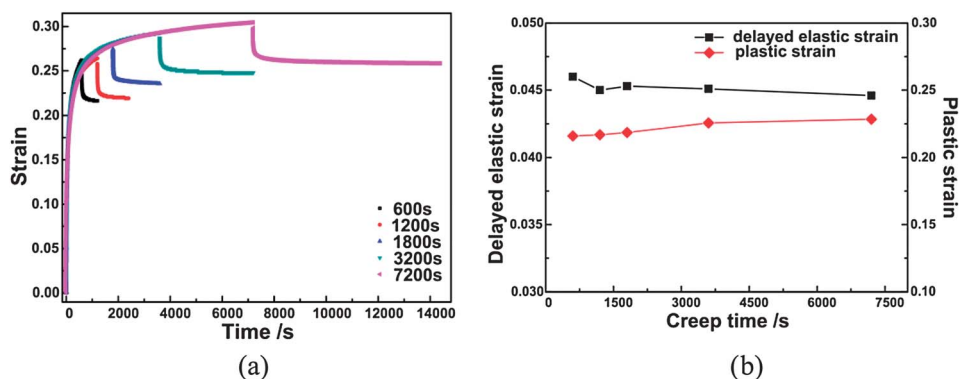


Fig. 2 The creep and recovery curves (a), delayed elastic strains, and plastic strain (b) of MRP under a 930 mT magnetic field and a 20 kPa constant shear stress at different creep times.

different creep time (Fig. 2b). It can also be seen from Fig. 2a that the viscous flow component is small in comparison to the residual strain (taking up an average 5.4% of residual strain). So it can be deduced that the residual strain is dominated by plastic strain. The plastic strain mainly generates in the primary creep process because its value keeps almost constant after the MRP enters the secondary creep stage (Fig. 2a). The cause of plastic deformation may originate from the slipping between soft chain segments and iron particles.

According to the above analysis, taking 1800 s as the creep and recovery time is long enough to read the key information from the creep and recovery curves. If needed, Burger's model can be introduced to predict the creep process at longer time.

3.2. Determination of constant stress level

Constant stress level is another important influence factor on the creep and recovery behaviors for viscoelastic materials.³² As a kind of magneto-sensitive smart material, a magnetic field will play a critical role in the creep and recovery behaviors of MRP, so a series of creep and recovery experiments under various constant stresses were conducted with and without a magnetic field, respectively (Fig. 3 and Fig. 4). The influence of magnetic field strength on the creep and recovery behaviors will be discussed in detail later. Here, we firstly concentrate on the influence of the stress level and analyze the discrepancies between the response strains of MRP at various constant stresses with and without magnetic field.

The creep and recovery behaviors of MRP with and without magnetic field are quite different. When the stress is lower than a certain value, the primary and secondary creep stage can be observed clearly from Fig. 4a and b while the response strain is proportional to creep time in the absence of magnetic field (Fig. 3a and b). In addition, the response strain without a magnetic field is much greater than that with magnetic field under the same applied constant stress of 2000 Pa (as shown in Fig. 3a and 4a). However, with the increase of a constant stress level, the response strain will increase accordingly, whether or not an external magnetic field is applied to MRP. When the constant stress increases to a critical value, the tertiary creep stage appears which means creep rupture occurs. As time goes

by, the response strain increases sharply, implying that the rotor may separate with MRP and the strain is invalid.

For linear materials, the stress-strain curves at constant time (isochron) are straight lines. Or else, the materials are nonlinear. That is to say, the creep compliance is dependent on stress level for nonlinear materials.³³ Before the creep rupture occurs, the creep compliances of MRP at different constant stress without and with magnetic field were calculated, which are shown in Fig. 3d and 4d, respectively. It can be seen that the creep compliance increases with the increasing stress level at the same creep time (Fig. 3d and 4d), indicating that the MRP is a complex nonlinear material at the selected stress range and this nonlinearity seems not to be affected by magnetic field. The nonlinearity of MRP may be attributed to the movements of chain segments in polyurethane and the magnetic-mechanical coupling effects between iron particles and matrix. For the MRP without a magnetic field, when the constant stress increases to 10 kPa, the response strain is proportional to creep time for an initial 100 s, then an accelerating strain rate is observed (the inset of Fig. 3c), indicating that MRP undergoes a tertiary creep stage. Finally, a sharp increase of response strain is detected. In contrast, the critical constant stress which can cause the tertiary creep for MRP with a 930 mT magnetic field is larger (32 kPa) and the start point of tertiary creep stage is smaller (about 64 s). In addition, the primary creep stage can be observed from the inset of Fig. 4c. The appearance of tertiary creep is ascribed to the microstructure rupture of MRP. To sustain a large enough constant stress, a large deformation process will generate. The stretching effects of chain segments in MRP and the rubbing effects between them during the deformation process are the deformation mechanism for resisting external stress. As time goes by, the stretching effects will fade since more and more chain segments can not be stretched further. In this case, the deformation will accelerate to make rubbing effects (which are relevant to deformation rate) strengthen, and then the tertiary creep appears. However, the torsion force will exceed the static frictional force between rotator and material surface if the deformation rate is too large, resulting in a separation of rotor and material surface. The dramatically increasing strain recorded after the separation of rotor and material surface is meaningless (Fig. 3c). When a magnetic field is applied, the magnetic interactions between iron particles will contribute to the resistance to external force, which

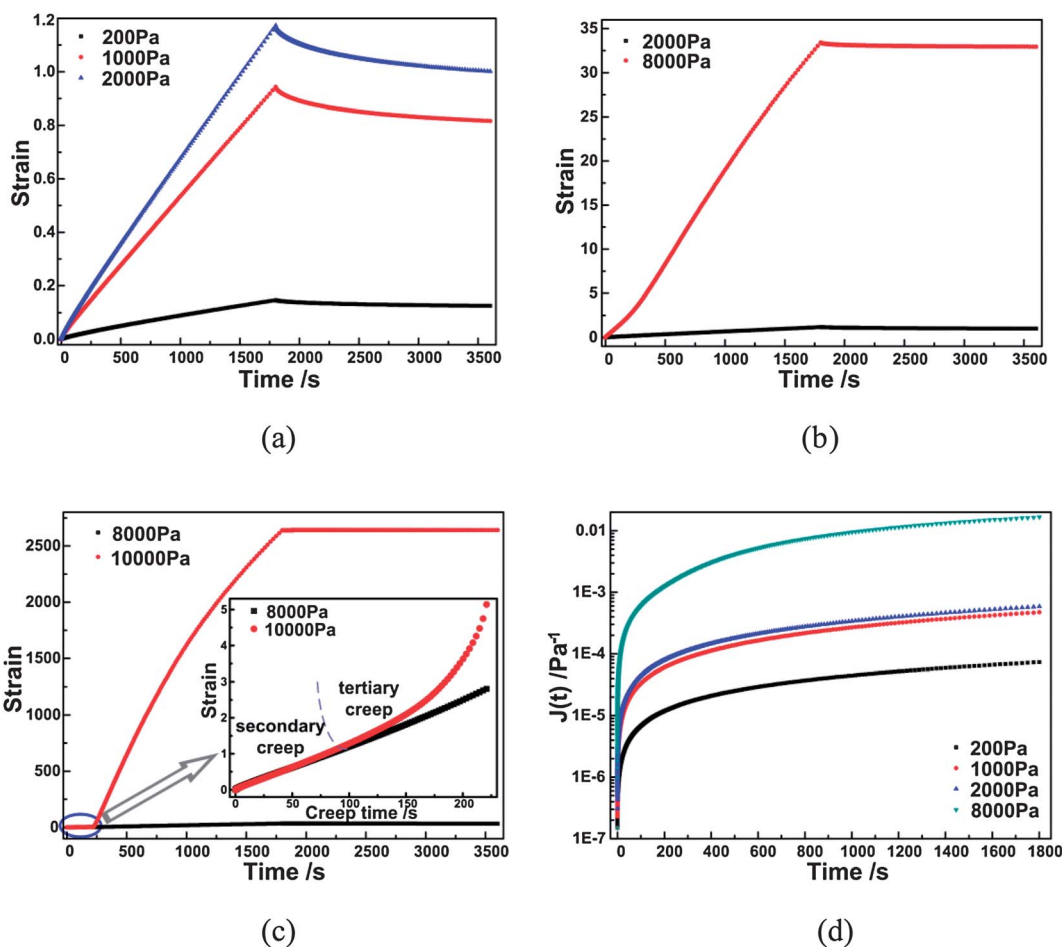


Fig. 3 The creep and recovery curves (a), (b), (c) and creep compliance (d) of MRP under various constant stresses in the absence of magnetic field.

will raise the critical stress for creep rupture (32 kPa with a 930 mT magnetic field). At the same time, magnetic field will make the MRP stiffer and the magnetic interactions between iron particles will restrict the movements of chain segments in the matrix, which will shorten the start time of the tertiary creep. The generation of tertiary creep implies structure rupture of MRP and this should be avoided in characterization or some applications for MRP. Therefore, 2000 Pa was chosen as the applied stress to avoid the creep rupture at the setting creep time.

3.3. The influence of magnetic field on creep and recovery behaviors

Magnetic-controllability is the most important and fascinating property for MR materials. Fig. 5a, b, and c show the dependence of magnetic field on the creep and recovery behaviors of MRP under a constant stress of 2000 Pa. The creep strain decreases sharply with an increase of the magnetic field at the creep time of 1800 s. For instance, the creep strain of MRP without a magnetic field is 176 times larger than that of MRP with a 930 mT magnetic field and this ratio will be larger with the increasing of creep time. This result proves that the magnetic field can make MRP become stiffer from the perspective of time-dependent mechanical behaviors. Three figures (Fig. 5a, b, and c) were used with linear coordinates to illuminate the creep

and recovery behaviors of MRP under different magnetic field, from which the details of influence of magnetic field can be analyzed explicitly. At the same time, the creep compliances calculated from the experimental results (Fig. 5a, b, and c) are presented in Fig. 5d with the vertical logarithmic coordinate based on log 10 so that the whole effect of magnetic field in a wide range on creep behavior of MRP can be demonstrated clearly.

Except for the influence on the value of creep strain, the physical state of MRP can also be changed by magnetic field. It can be seen from Fig. 5a that the creep strain is proportional to time without magnetic field, indicating the second creep region dominates in this condition and the MRP behaves like a viscous liquid. However, after the constant shear stress is removed the creep strain can be recovered partly, which indicates that the delayed elastic strain generates even when there is no apparent primary creep region. Therefore, MRP can not simply be regarded as a viscous liquid though the response strain increases linearly with time in the creep stage (there is no recoverable strain generates after the unloading for ideal viscous fluids). With increasing magnetic field (Fig. 5a, b, and c), on the one hand, the creep strain decreases dramatically at the same creep time; on the other hand, the creep curves bend downwards with time, indicating that the primary creep stage that contains delayed elastic strain generates and the proportion of it in the

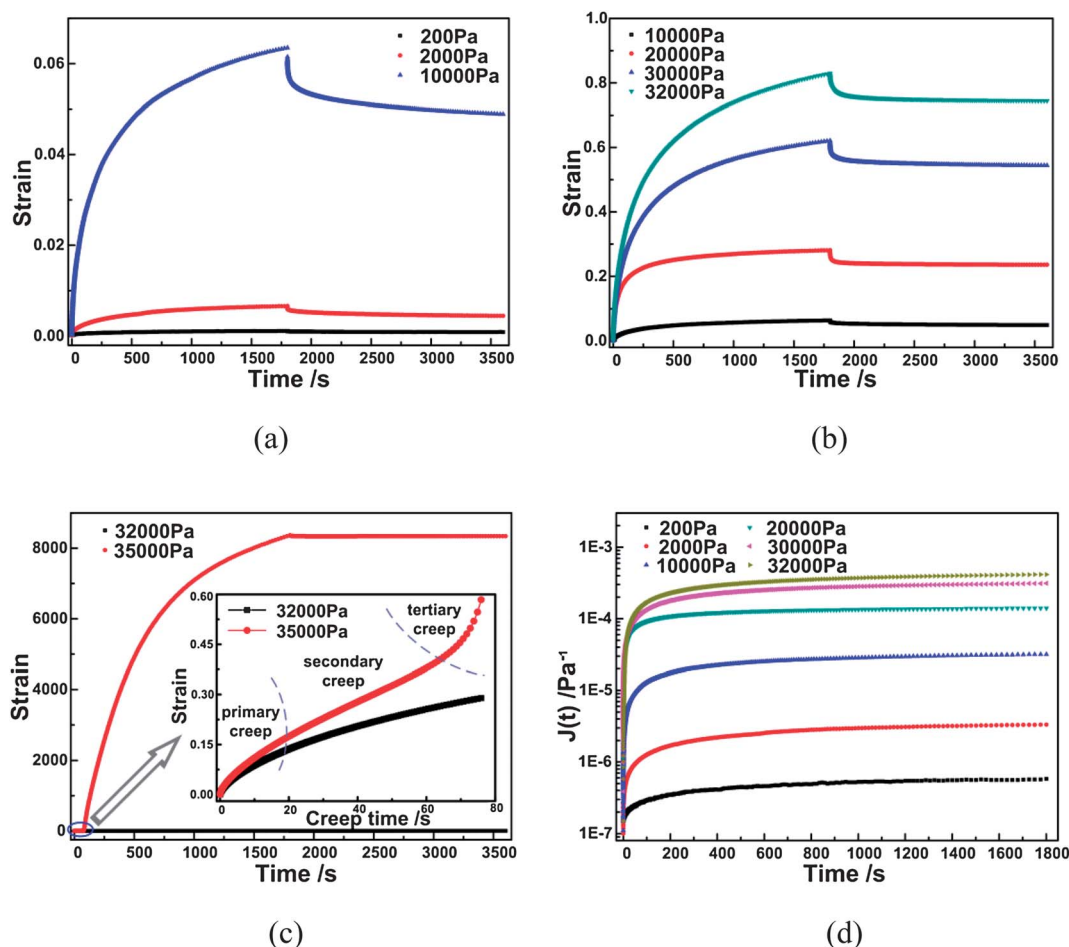


Fig. 4 The creep and recovery curves (a), (b), (c) and creep compliance (d) of MRP under various constant stresses with a 930 mT magnetic field.

creep strain increases with the increasing magnetic field. At the same applied constant stress, the influence of magnetic field in a wide range on the creep behavior can also be characterized by the creep compliance which is proportional to response strain. As illustrated in Fig. 5d, it is clear that the creep compliance decreases gradually with the increasing magnetic field at the same creep time. Further, the residual strain can be calculated from the recovery curves (Fig. 5a, b, and c). Ultimately, the delayed elastic strain and the ratio of delayed elastic strain to the total strain at the creep time of 1800 s with different magnetic field can be obtained (Fig. 6). The delayed elastic strain decreases sharply with the increasing magnetic field at first and then tends to level off. Interestingly, the ratio of elastic strain shows an opposite tendency. This is because the total strain decreases with magnetic field even more sharply than the delayed elastic field. For example, the ratio of total strain without magnetic field to the total strain with a 930 mT magnetic field is 176.1 while the same ratio for delayed elastic strain is 62.4. The ratio of residual strain to the total strain in the absence of magnetic field at the creep time of 1800 s is 88.41%, indicating that the residual strain plays a dominate role in response to the applied constant stress. The above results further prove that the MRP is a solid-like MR gel, which behaves like plasticine in the absence of magnetic field.

The creep behaviors are mainly attributed to the movements of soft chain segments of polyurethane in MRP. There are two movement manners for the soft chain segments; one is the stretching, which is relevant with delayed elastic strain, another is the slipping, which leads to residual stain. After the constant stress is removed, the stretching soft chain segments will convolute at long enough time. Therefore, the creep strain can recover partly because of the convolution of soft chain segments. As for this plastic MRP, the slipping between the soft chain segments is the major response mechanism when applying a constant stress to it without magnetic field. Both stretching and convolution phenomena also occur in the creep and recovery stage respectively. Consequently, the response strain increases linearly with time under a constant shear stress and partly recovers after unloading. When MRP is subjected to magnetic field, the iron particle chains will become rigid, which will restrict the movements of the soft chain segments. At the macro perspective, this microscopic restriction effect can be represented as the creep strain which decreases with an increase of the magnetic field. It can be deduced from Fig. 5 that the magnetic-induced restriction effect is huge in the initial increasing stage of magnetic field, and with an increase of magnetic field, the restriction effect tends to saturation. In addition, the restriction effects to the slipping of soft chain segments become larger than

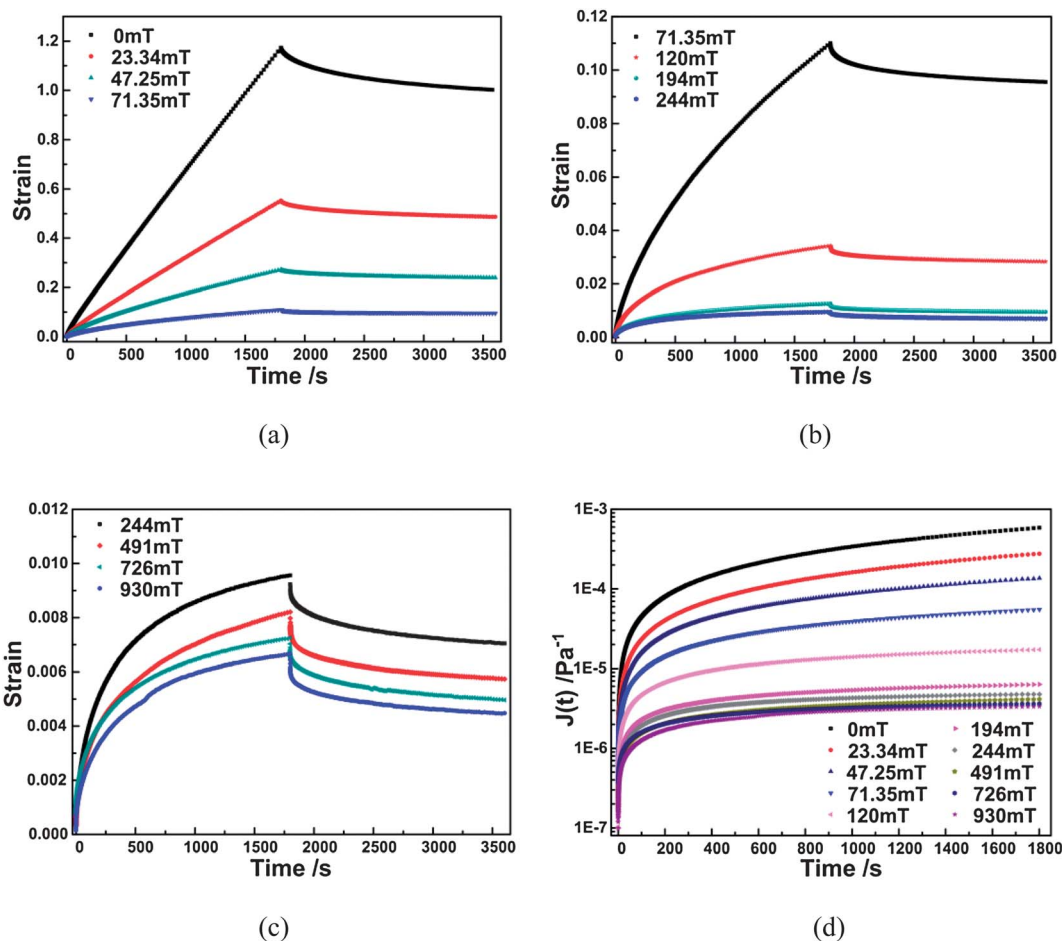


Fig. 5 The creep and recovery curves (a), (b), (c) and creep compliance (d) of MRP under a constant stress of 2000 Pa and different magnetic field.

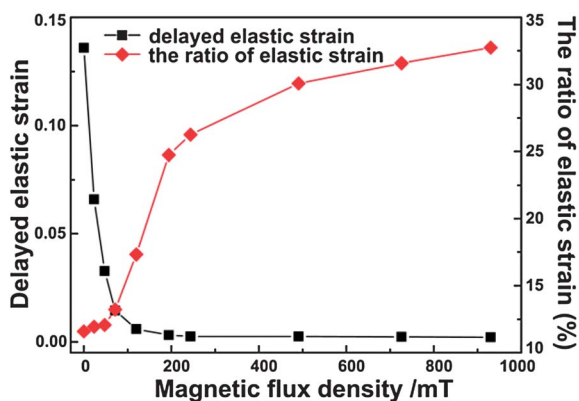


Fig. 6 Delayed elastic strain and the ratio of elastic strain to the total strain under different magnetic field at the creep time of 1800 s. Delayed elastic strain and the total strain were calculated from the recovery curves of MRP under different magnetic fields (Fig. 5a, b, and c) and Weibull distribution function (eqn (4)).

those to the stretching and convolution of soft chain segments with the increasing magnetic field, which makes the physical state of MRP change from viscoplastic to elasticplastic (the ratio of delayed elastic strain changes from 11.6% to 32.7% when the magnetic field increases from 0 to 930 mT, as shown in Fig. 6).

3.4. The influence of particle distribution on the creep and recovery behaviors

The iron particles in these solid-like MR gels can be rearranged by magnetic field and their locations can be kept even after removing the magnetic field. Therefore, the mechanical properties may be changed if the particle distribution is changed, which is a unique and fascinating property for these solid-like MR gels.²⁸ Here, the time-dependent mechanical properties of MRP with different particle distributions were discussed. Creep and recovery experiments were carried out on two kinds of MRP samples (with different particle distribution: isotropic MRP and anisotropic MRP) without (Fig. 7a) and with (Fig. 7b) magnetic field, respectively.

Without a magnetic field, both the isotropic MRP and the anisotropic MRP behave like a viscous liquid in the creep stage and the creep strain can recover partly after the constant shear stress is removed. The difference is the creep strain ($=2.73785$) and delayed elastic strain ($=0.259$) of isotropic MRP is larger than those (1.1728 and 0.172, respectively) of anisotropic MRP at the same creep time, respectively (as shown in Fig. 7a). This indicates that the restriction effects of MRP with chain-like particle distribution to the movements of soft chain segments are larger than those of MRP with random particle distribution.

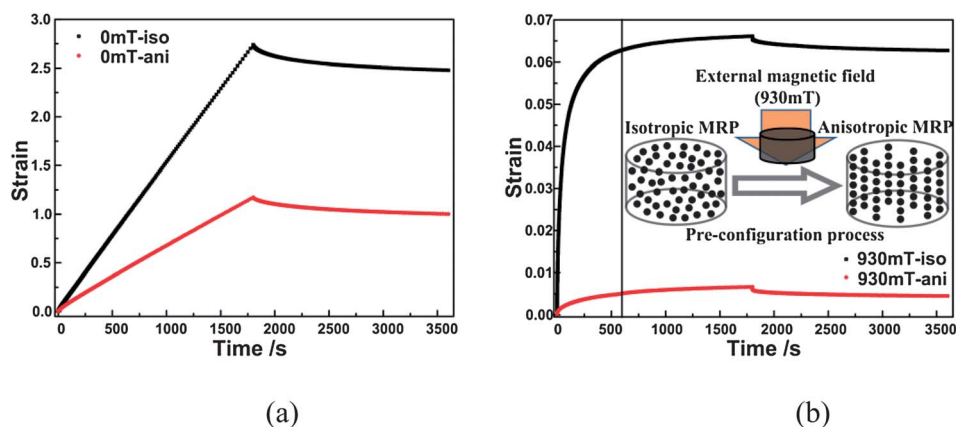


Fig. 7 The creep and recovery curves for two kinds of MRP without (a) and with (b) magnetic field at a constant stress of 2000 Pa. The “0 mT” after the legend represents no magnetic field during the experiment process while the “930 mT” after the legend represents a 930 mT magnetic field, which was applied to the sample during the experiment process. The “iso” after the legend represents isotropic MRP while the “ani” represents anisotropic MRP.

Fig. 7b shows the response strains of isotropic MRP and anisotropic MRP to the applied stress with a magnetic field of 930 mT. Due to the magnetic-induced restriction effects, the response strains of MRP with magnetic field are far less than those of MRP without a magnetic field. For the same reason, the creep behavior of isotropic MRP at the initial creep stage is quite different from that of anisotropic MRP. It can be observed from Fig. 7b that the creep strain of isotropic MRP shows a sharp increase with time at the initial creep stage. When the response time exceeds 600 s, the creep and recovery behaviors for the two kinds of MRP are almost the same. At the beginning of the creep test, the iron particles of isotropic MRP are dispersed in the matrix randomly (inset of Fig. 7b). When the isotropic MRP is subjected to an external magnetic field, the iron particles will rearrange along the direction of magnetic field and form a stable chain-like or column-like structure. This kind of MRP with stable chain-like or column-like structure is what we called anisotropic MRP. It is not difficult to understand that the magnetic-induced restriction effects of the matrix for MRP with different configurations are different. The anisotropic MRP with larger magnetic interactions will induce stronger restriction effects to the matrix, and a smaller response strain will be caused under the same constant stress. A pre-configuration process of MRP can be actually reflected from the creep curves in the time range from 0 s to 600 s. During the pre-configuration process, the microstructure of isotropic MRP is unstable, which will generate smaller magnetic interactions in comparison with the anisotropic MRP with a stable microstructure, where a larger response strain will be caused. After 600 s, the pre-configuration of isotropic MRP is complete and the creep and recovery curves are identical because the isotropic MRP has changed into anisotropic MRP. This is the reason why we chose 10 min as the pre-configuration time.

3.5. Temperature effect on the creep behavior

The temperature dependence of MRP on the creep behavior is illustrated in Fig. 8. It can be seen from Fig. 8a that the creep strain decreases with an increase of the temperature at the same creep time, indicating that the MRP becomes stiffer when

subjected to a 930 mT magnetic field. This is quite different from the results obtained from MR fluids and MR elastomers. A temperature thinning effect was found in MR fluids^{14,34,35} and a similar phenomenon was also observed from MR elastomers.³⁶ In comparison, the creep experiments of MRP without a magnetic field at different temperatures were performed (as shown in Fig. 8b). In this situation, the creep behaviors of MRP in the absence of a magnetic field are contrary to those with a magnetic field of 930 mT.

Based on these experimental results, it is deduced that the increase of modulus of MRP under a 930 mT magnetic field with increasing temperature mainly originates from the magnetic interactions between iron particles and the coupling effects between the matrix and iron particle chains. Here, a time-dependent parameter ($G(t)$) is defined to describe the ability of resisting deformation for MRP in the creep stage. The relationship of constant stress, the creep strain, and $G(t)$ and the components of $G(t)$ can be represented as follow:

$$\tau_0 = G(t) \cdot \gamma_T(t) \quad (5)$$

$$G(t) = G_{\text{magnetic}} + G_{\text{matrix}}(t) + G_{\text{coupling}}(t) \quad (6)$$

In fact, $G(t)$ is the reciprocal of $J(t)$, which can be named as creep modulus. It is assumed that $G(t)$ is contributed to by three parts, as shown in eqn (6), where G_{magnetic} denotes the effects of magnetic interactions between iron particles, $G_{\text{matrix}}(t)$ represents the contribution to $G(t)$ by the matrix part, and $G_{\text{coupling}}(t)$ is the coupling effect between the matrix and iron particles chains. It is necessary to note that G_{magnetic} does not vary with time but is associated with temperature. $G_{\text{coupling}}(t)$ is a negative value, which is used for describing the restriction effects of matrix to iron particle chains. That is to say, it will weaken the resistance effects of magnetic interactions to external stress. The matrix will become softer with the increase of temperature, indicating that $G_{\text{matrix}}(t)$ will diminish. At the same time, the soft matrix will weaken the restriction effects to iron particle chains, resulting in the increment of $G_{\text{coupling}}(t)$. The orientation of particles aligned with the direction of the magnetic field will become easier due to the weaker restriction effects from the

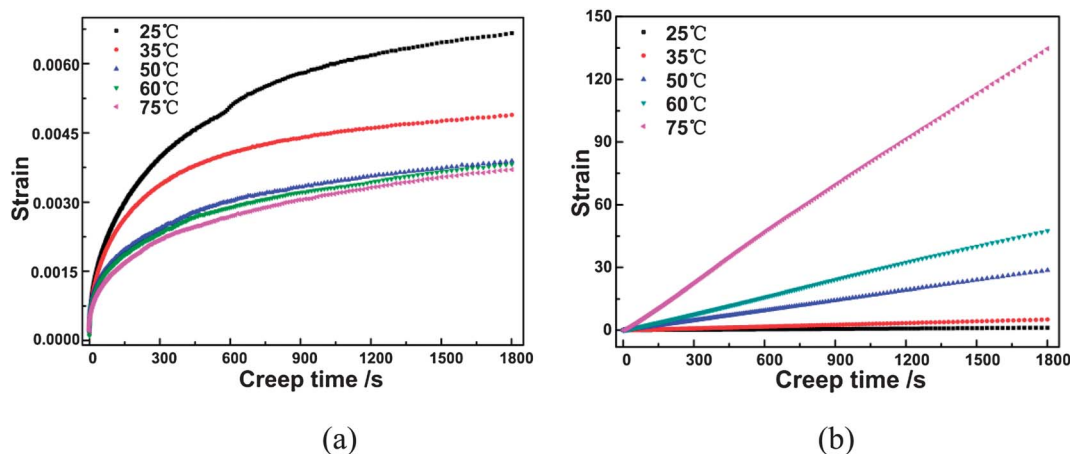


Fig. 8 The creep and recovery curves of MRP under a 2000 Pa constant stress with a 930 mT magnetic field (a) and in the absence of magnetic field (b) at different temperatures.

matrix. Therefore, the degree of anisotropy of MRP will increase with the increasing temperature, in other words, the increasing temperature will lead to the increase of G_{magnetic} . By contrast, the increasing amount of $G_{\text{coupling}}(t)$ and G_{magnetic} are larger than the decrease of $G_{\text{matrix}}(t)$, which causes the increase of $G(t)$. Consider eqn (5), to keep the constant stress the creep strain will decrease with the increasing temperature because of the increase of $G(t)$. For Fig. 8b, where the creep curves were tested without a magnetic field, $G(t) = G_{\text{matrix}}(t)$. In this situation, $G_{\text{matrix}}(t)$ will decrease with the increasing temperature, indicating that the creep strain will increase with the increasing temperature. This is consistent with the experimental results (Fig. 8b).

4. Conclusions

In this work, the creep and recovery behavior of MRP under various experimental conditions were studied. By increasing the magnetic field, the creep strain decreases sharply at the same creep time, indicating that the magnetic field can make MRP become stiffer. The creep strain of isotropic MRP increases more sharply than the creep strain of anisotropic MRP under a 930 mT magnetic field at the initial 10 min. Without the magnetic field, the MRP behaves like a viscous liquid at the creep stage. When a magnetic field is applied to MRP, the creep curves bend downwards with time, indicating that the primary creep stage generates and the proportion of elastic strain increases with the increasing magnetic field. The tertiary creep stage, which means the appearance of creep rupture, will appear if the applied constant stress increases to the critical value and the critical value of constant stress is highly influenced by the magnetic field. Interestingly, the creep strain decreases with increasing temperature when subjected to a magnetic field of 930 mT, which has not been found for other MR materials. In comparison, the creep strain for MRP without a magnetic field increases with increasing temperature. Therefore, it is concluded that the temperature effect on the creep behavior of MRP with magnetic field may originate from the magnetic interactions between iron particles and the coupling effects between the matrix and iron particle chains.

Acknowledgements

Financial support from the National Natural Science Foundation of China (grant nos. 11125210, 11072234, 11102202), the National Basic Research Program of China (973 Program, grant no. 2012CB937500) and the Specialized Research Fund for the Doctoral Program of Higher Education of China (Project no.20093402110010) are gratefully acknowledged.

References

- 1 H. Watanabe, T. Inoue and Y. Matsumiya, *Macromolecules*, 2006, **39**, 5419.
- 2 P. Barai and G. J. Weng, *Acta Mech.*, 2008, **195**, 327.
- 3 Y. M. Joshi, *Ind. Eng. Chem. Res.*, 2009, **48**, 8232.
- 4 M. Kraft, J. Meissner and J. Kaschta, *Macromolecules*, 1999, **32**, 751.
- 5 P. W. Majsztrik, A. B. Bocarsly and J. B. Benziger, *Macromolecules*, 2008, **41**, 9849.
- 6 H. Muenstedt, N. Katsikis and J. Kaschta, *Macromolecules*, 2008, **41**, 9777.
- 7 X. Wu, R. E. Sallach, J. M. Caves, V. P. Conticello and E. L. Chaikof, *Biomacromolecules*, 2008, **9**, 1787.
- 8 K. Oh, M. Jemmett and M. Deo, *Ind. Eng. Chem. Res.*, 2009, **48**, 8950.
- 9 Y. Jia, K. Peng, X. L. Gong and Z. Zhang, *Int. J. Plast.*, 2011, **27**, 1239.
- 10 R. A. Riggleman, K. S. Schweizer and J. J. de Pablo, *Macromolecules*, 2008, **41**, 4969.
- 11 V. Awasthi and Y. M. Joshi, *Soft Matter*, 2009, **5**, 4991.
- 12 B. Baldewa and Y. M. Joshi, *Soft Matter*, 2012, **8**, 789.
- 13 H. Hilles and F. Monroy, *Soft Matter*, 2011, **7**, 7790.
- 14 W. H. Li, H. Du, G. Chen and S. H. Yeo, *Mater. Sci. Eng., A*, 2002, **333**, 368.
- 15 J. de Vicente, M. T. Lopez-Lopez, F. Gonzalez-Caballero and J. D. G. Duran, *J. Rheol.*, 2003, **47**, 1093.
- 16 H. See, R. Chen and M. Keentok, *Colloid Polym. Sci.*, 2004, **282**, 423.
- 17 W. H. Li, Y. Zhou, T. F. Tian and G. Alici, *Front. Mech. Eng. China*, 2010, **5**, 341.
- 18 T. Shiga, A. Okada and T. Kurauchi, *J. Appl. Polym. Sci.*, 1995, **58**, 787.
- 19 M. J. Wilson, A. Fuchs and F. Gordaninejad, *J. Appl. Polym. Sci.*, 2002, **84**, 2733.
- 20 A. Fuchs, M. Xin, F. Gordaninejad, X. J. Wang, G. H. Hitchcock, H. Gecol, C. Evrensel and G. Korol, *J. Appl. Polym. Sci.*, 2004, **92**, 1176.
- 21 A. Fuchs, B. Hu, F. Gordaninejad and C. Evrensel, *J. Appl. Polym. Sci.*, 2005, **98**, 2402.
- 22 B. Hu, A. Fuchs, S. Huseyin, F. Gordaninejad and C. Evrensel, *J. Appl. Polym. Sci.*, 2006, **100**, 2464.

-
- 23 T. Mitsumata, T. Wakabayashi and T. Okazaki, *J. Phys. Chem. B*, 2008, **112**, 14132.
- 24 B. Wei, X. L. Gong, W. Q. Jiang, L. J. Qin and Y. C. Fan, *J. Appl. Polym. Sci.*, 2010, **118**, 2765.
- 25 H. N. An, S. J. Picken and E. Mendes, *Soft Matter*, 2010, **6**, 4497.
- 26 T. Mitsumata and S. Otori, *Polym. Chem.*, 2011, **2**, 1063.
- 27 J. K. Wu, X. L. Gong, Y. C. Fan and H. S. Xia, *Soft Matter*, 2011, **7**, 6205.
- 28 Y. G. Xu, X. L. Gong, S. H. Xuan, W. Zhang and Y. C. Fan, *Soft Matter*, 2011, **7**, 5246.
- 29 R. W. Whorlow, *Rheological Techniques*, Ellis Horwood, 1992.
- 30 W. N. Findley, J. S. Lai and K. Onaran, *Creep and Relaxation of Nonlinear Viscoelastic Materials: With an Introduction to Linear Viscoelasticity*, Courier Dover Publications, New York, 1989.
- 31 K. S. Fancey, *J. Mater. Sci.*, 2005, **40**, 4827.
- 32 F. Gobeaux, E. Belamie, G. Mosser, P. Davidson and S. Asnacios, *Soft Matter*, 2010, **6**, 3769.
- 33 R. Lakes, *Viscoelastic Materials*, Cambridge University Press, 2009.
- 34 F. Gordaninejad and D. G. Breese, *J. Intell. Mater. Syst. Struct.*, 1999, **10**, 634.
- 35 F. Zschunke, R. Rivas and P. O. Brunn, *Appl. Rheol.*, 2005, **15**, 116.
- 36 W. Zhang, X. L. Gong, S. H. Xuan and W. Q. Jiang, *Ind. Eng. Chem. Res.*, 2011, **50**, 6704.